

RESEARCH

Open Access



Wave propagation in a transversely isotropic microstretch elastic solid

Baljeet Singh*  and Manisha Goyal

Abstract

Background: The theory of microstretch elastic bodies was first developed by Eringen (1971, 1990, 1999, 2004). This theory was developed by extending the theory of micropolar elasticity. Each material point in this theory has three deformable directors.

Methods: The governing equations of a transversely isotropic microstretch material are specialized in x-z plane. Plane wave solutions of these governing equations results into a bi-quadratic velocity equation. The four roots of the velocity equation correspond to four coupled plane waves which are named as Coupled Longitudinal Displacement (CLD) wave, Coupled Longitudinal Microstretch (CLM) wave, Coupled Transverse Displacement (CTD) wave and Coupled Transverse Microrotational (CTM) wave. The reflection of Coupled Longitudinal Displacement (CLD) wave is considered at a stress-free surface of half-space of material. The appropriate displacement components, microrotation component and microstretch potential for incident and four reflected waves in half-space are formulated. These solutions for incident and reflected waves satisfy the boundary conditions at a stress free surface of half-space and we obtain a non-homogeneous system of four equations in four reflection coefficients (or amplitude ratios) along with Snell's law for the present model.

Results: The speeds of plane waves are computed by Fortran program of bi-quadratic velocity equation for relevant physical constants of the material. The reflection coefficients of various reflected waves are also computed by Fortran program of Gauss elimination method. The speeds of plane waves are plotted against angle of propagation direction with vertical axis. The reflection coefficients of various reflected waves are plotted against the angle of incidence. These variations of speeds and reflection coefficients are also compared with those in absence of microstretch parameters.

Conclusions: For a specific material, numerical simulation in presence as well as in absence of microstretch shows that the coupled longitudinal displacement (CLD) wave is fastest wave and the coupled transverse microrotational (CTM) is observed slowest wave. The coupled longitudinal microstretch (CLM) wave is an additional wave due to the presence of microstretch in the medium. The presence of microstretch in transversely isotropic micropolar elastic solid affects the speeds of plane waves and the amplitude ratios of various reflected waves.

2010 Mathematics Subject Classification: 74J

Keywords: Transverse isotropy, Microstretch, Microrotation, Plane waves, Reflection coefficients

Background

The linear theory of elasticity has numerous applications in engineering structural materials. The linear elasticity describes the mechanical behaviour of concrete, wood and coal. However, the linear theory of elasticity does not describe the behaviour of some new synthetic

materials, for example, polymethyl-methacrylate, polyethylene, polyvinyl chloride. The behaviour of such material is described by the theory of micropolar elasticity. Eringen (1999, 2001) stated that "the range of possible materials to be modelled by micropolar theory is very wide. It includes anisotropic fluids, liquid crystals with rigid molecules, rigid suspensions, magnetic fluids, clouds with dust, muddy fluids, biological fluids, animal blood with rigid cells, chopped fiber composites, bones, concrete with

*Correspondence: bsinghgc11@gmail.com
Department of Mathematics, Post Graduate Government College, Sector-11,
160 011 Chandigarh, India

sand". In elastic vibrations of high frequencies (20 kHz–1000 kHz) and small wavelengths, the effect of the microstructure in a body becomes prominent. Micropolar continua is treated as a special case of microstretch continua and the microstretch continua is treated as special case of micromorphic continua. Eringen (1999, 2001) developed these microcontinuum field theories. In contrast to classical continuum mechanics, the material particles in these microcontinuum theories undergo an additional micromotion corresponding to the rotation and deformation of the material particle at the microscale. Most of experimental research presented in aspects of composite materials, micromechanics, cellular solids, and biological materials may be understood via Cosserat or Micropolar elasticity. Eringen (1999, 2001) states, "experiments with micropolar constants require much precision and elaborate instrumentation, since we are faced with the measurement of microscopic-level quantities in high frequency, short-wavelength regions. Therefore, experimental work using micropolar theory as a basis for the design of experimental setups (in order to measure at least some of the many material parameters) and the interpretation of measured data is still very rare". Few promising experimental results are available in the literature, for example, Askar (1972), Bazant and Christensen (1972), Gauthier and Jashman (1975), Fischer-Hjalmars (1981, 1982), Gauthier (1982), Yang and Lakes (1982), Pouget et al. (1986) and Kiris and Inan (2008). Various other experimental studies in micropolar continuum are done by using micromechanical approach. For example, Lakes (1991), De Bellis and Addessi (2014), Niu and Yan (2016) and Hassonpour and Heppler (2017).

The theory of microstretch elastic bodies was first developed by Eringen (1971, 1990, 1999, 2004). This theory was developed by extending the theory of micropolar elasticity. Each material point in this theory has three deformable directors. A body is treated as a microstretch medium when the directors are restricted with breathing-type microdeformations only. Also, the material points of a microstretch solid possess the property of stretching and contracting independently of their translations and rotations. This theory removed the shortcomings between classical elasticity and experiments. The classical elasticity is unable to show the effects of material microstructure, which contribute significantly to the overall deformations in a body. For an instance, as stated by Eringen (1999), "the classical theory of elasticity fails to produce acceptable results in the cases of polymers, graphite, asphalt, human bones, composite materials reinforced with chopped elastic fibres and porous media saturated with gas or inviscid liquid". Due to the importance of small-scale effects in the prediction of the overall mechanical behaviour of these materials, these help in designing and manufacturing of modern day advanced materials.

Various problems based on the Eringen's theory of microstretch elasticity are studied by many authors. For example, Iesan and Pompei (1995) presented a solution of Boussinesq Somigliana Galerkin type for the boundary value problem in static theory of microstretch elasticity and established existence and uniqueness results. Ciarletta (1999) investigated the isothermal bending of microstretch elastic plates. Kumar et al. (2003) studied plane strain problem in a microstretch solid. Marin (2010) presented a domain of influence theorem in microstretch materials. Kiris and Inan (2008) estimated microstretch elastic moduli of materials by using vibration data of plates. Various problems on plane and surface waves in isotropic microstretch elastic materials are studied by many authors. For instance, Nowinski (1993) particularized the general field equations governing the propagation of a nonlocal surface wave and examined the propagation of a microrotation and microstretch wave in a nonlocal medium. Singh (2002) studied the the plane waves in an isotropic microstretch elastic solid and discussed a problem on reflection of the plane waves from free surface to obtain the reflection coefficients and energy ratios of reflected waves. Kumar et al. (2004) discussed a problem on the Rayleigh waves in an isotropic microstretch thermoelastic diffusion solid half space. Sharma et al. (2007, 2009) considered the problems on propagation of Rayleigh surface waves in an isotropic microstretch continua with effects of micropolarity and relaxation times. Sharma et al. (2014) studied the plane waves in an isotropic electromicrostretch elastic solid. Othman and Jahangir (2015) studied the effects of rotation and temperature dependent elastic properties on the speed of plane waves in an isotropic microstretch medium. Singh et al. (2016) considered the reflection and transmission of dilatational waves at a microstretch solid/fluid interface.

Metallic components (like single crystals or polycrystalline components) with dominant orientation in crystals in the microstructure material exhibit highly anisotropic properties. Seismic anisotropy provides important information regarding structure of the sedimentary rocks and helps in better understanding of the earth. Wave propagation in anisotropic solids has three important features (a) wave velocity variation with direction of propagation (b) three-dimensional displacement of the particle and (c) energy propagation deviated both in velocity and direction from phase propagation. In each propagation direction, the bulk waves propagate in isotropic materials with equal velocity at each angle of propagation. But in anisotropic materials, elastic waves propagate with a velocity which depends on direction. There are various studies on modelling of elastic waves in transversely isotropic composites. For example, Rytov (1956), Abubakar (1962), Keck and Armenkas (1971), Daley and Hron (1977), Payton (1992), Kushwaha et al. (1993),

Suvalov et al. (2005), Rudykh and deBotton (2012), Rudykh and Boyce (2014) and Galich et al. (2016, 2017). Some problems on wave propagation in transversely isotropic micropolar medium have been investigated by various authors. For example, Gupta and Kumar (2009), Kumar and Gupta (2010a, 2010b, 2012) and Abbas and Kumar (2014). In these problems, numerical values of speeds and reflection coefficients are computed with the help of an arbitrarily chosen data.

The problems on waves and vibration in transversely isotropic elasticity of microstretch material are not studied much in literature. For an instance, Singh et al. (2015) derived the governing equations for transversely isotropic microstretch elastic solid and solved a problem on Rayleigh wave propagation along the half-space of the material. Plane wave propagation in transversely isotropic microstretch elastic solid is not reported in literature yet. This paper considers the plane wave propagation in a transversely isotropic microstretch elastic medium. The basic equations of motion for a transversely isotropic microstretch elastic solid are formulated and solved for plane wave solutions. A bi-quadratic velocity equation for possible plane waves in the medium is obtained. A non-homogeneous system of four equations in reflection coefficients (or amplitude ratios) are obtained for incident CLD wave. The speeds of plane waves and reflection coefficients are computed and plotted to observe the effects of microstretch parameters.

Governing equations

Following Eringen (1971, 1990, 1999, 2004), the basic equations of linear theory of microstretch elasticity are:

$$t_{ij} = \rho \ddot{u}_i, \quad (1)$$

$$m_{ik,i} + \epsilon_{ijk} t_{ij} = \rho j \ddot{\phi}_k, \quad (2)$$

$$\pi_{k,k} - \sigma = j_0 \ddot{\Phi} \quad (3)$$

$$t_{ij} = A_{ijrs} e_{rs} + B_{ijrs} \kappa_{rs} + D_{ij} \Phi + F_{ijk} \zeta_k \quad (4)$$

$$m_{ij} = B_{rsij} e_{rs} + C_{ijrs} \kappa_{rs} + E_{ij} \Phi + G_{ijk} \zeta_k \quad (5)$$

$$\sigma = D_{ij} e_{ij} + E_{ij} \kappa_{ij} + \zeta \Phi + h_k \zeta_k \quad (6)$$

$$\pi_k = F_{ijk} e_{ij} + G_{ijk} \kappa_{ij} + h_k \Phi + A_{kj}^* \zeta_j \quad (7)$$

$$e_{ij} = u_{j,i} + \epsilon_{jik} \phi_k, \quad \kappa_{ij} = \phi_{j,i}, \quad \zeta_j = \Phi_{,j} \quad (8)$$

Here, t_{ij} is the force stress tensor, m_{ij} is the couple stress tensor, ρ is the density, u_i are the components of the displacement vector, ϵ_{ijk} is the alternating tensor, ϕ_i are the components of the micro-rotation vector, π_k is the microstretch function, Φ is the microstress function, σ is the microinertia, j is the micro-inertia, j_0 is the microstretch inertia,

e_{ij} , κ_{ij} and ζ_k are the kinematic strain measures and A_{ijrs} , B_{ijrs} , C_{ijrs} , D_{ij} , E_{ij} , F_{ijk} , G_{ijk} , h_i , A_{ij} , κ_{ij} are constitutive coefficients. Latin subscripts range over the integers (1, 2, 3). Subscripts preceded by a comma denote partial differentiation with respect to the corresponding Cartesian coordinates. Superposed dot denotes partial differentiation with respect to the time t . The constitutive coefficients and the microinertia tensor are assumed to satisfy the following symmetry relations

$$\begin{aligned} A_{ijrs} &= A_{rsij}, \quad B_{ijrs} = B_{rsij}, \quad C_{ijrs} = C_{rsij}, \\ A_{ij} &= A_{ji}, \quad \kappa_{ij} = \kappa_{ji} \end{aligned} \quad (9)$$

Method

We consider a homogeneous transversely isotropic microstretch solid half space. We take the origin of the coordinates system on the free surface and negative z axis is pointing normally into the half-space, which is thus represented by $z \leq 0$. We assume that the medium is transversely isotropic in such a way that the planes of isotropy are perpendicular to z -axis. If we restrict our study to plane strain parallel to $x - z$ plane with displacement and microrotation vector of the form $u = (u_1, 0, u_3)$ and $\phi = (0, \phi_2, 0)$. With the help of Eqs. (4) to (9), the Eqs. (1) to (3) are specialized in $x - z$ plane as

$$\begin{aligned} A_{11} \frac{\partial^2 u_1}{\partial x^2} + (A_{13} + A_{56}) \frac{\partial^2 u_3}{\partial x \partial z} + A_{55} \frac{\partial^2 u_1}{\partial z^2} + K_1 \frac{\partial \phi_2}{\partial z} \\ + D_{11} \frac{\partial \Phi}{\partial x} = \rho \frac{\partial^2 u_1}{\partial t^2} \end{aligned} \quad (10)$$

$$\begin{aligned} A_{66} \frac{\partial^2 u_3}{\partial x^2} + (A_{13} + A_{56}) \frac{\partial^2 u_1}{\partial x \partial z} + A_{33} \frac{\partial^2 u_3}{\partial z^2} + K_2 \frac{\partial \phi_2}{\partial x} \\ + D_{33} \frac{\partial \Phi}{\partial z} = \rho \frac{\partial^2 u_3}{\partial t^2} \end{aligned} \quad (11)$$

$$\begin{aligned} B_{77} \frac{\partial^2 \phi_2}{\partial x^2} + B_{66} \frac{\partial^2 \phi_2}{\partial z^2} - K_1 \frac{\partial u_1}{\partial z} - K_2 \frac{\partial u_3}{\partial x} \\ - \chi \phi_2 = \rho j \frac{\partial^2 \phi_2}{\partial t^2} \end{aligned} \quad (12)$$

$$\begin{aligned} A_{11}^* \frac{\partial^2 \Phi}{\partial x^2} + A_{33}^* \frac{\partial^2 \Phi}{\partial z^2} - \xi \Phi - D_{11} \frac{\partial u_1}{\partial x} \\ - D_{33} \frac{\partial u_3}{\partial z} = j_0 \frac{\partial^2 \Phi}{\partial t^2} \end{aligned} \quad (13)$$

where $A_{11} = A_{1111}$, $A_{55} = A_{3131}$, $A_{13} = A_{1133} = A_{3311}$, $A_{56} = A_{3113} = A_{1331}$, $A_{66} = A_{1313}$, $A_{33} = A_{3333}$, $K_1 = A_{56} - A_{55} = A_{3113} - A_{3131}$, $K_2 = A_{66} - A_{56} = A_{1313} - A_{1331}$, $B_{77} = C_{1212}$, $B_{66} = C_{3232}$, $\chi = K_2 - K_1$.

Plane wave solution

We seek the plane wave solutions of Eqs. (10) to (13) in the following form

$$\{u_1, u_3, \phi_2, \Phi\} = \{A, B, C, D\} \exp \{ik(x \sin \theta + z \cos \theta - vt)\} \tag{14}$$

where θ is angle of propagation direction with vertical axis, k is wave number, v is the speed of wave and $\omega = kv$ is angular frequency.

Making use of Eq. (14) in Eqs. (10) to (13), we obtain four homogeneous equations in A, B, C and D , which have non-trivial solution if

$$\Gamma^4 - A^* \Gamma^3 + B^* \Gamma^2 - C^* \Gamma + D^* = 0 \tag{15}$$

Here $\Gamma = \rho v^2$, $A^* = D_1 + D_2 + D_3^* + D_4^*$, $B^* = D_1 D_2 + D_1 D_3^* + D_1 D_4^* + D_2 D_3^* + D_2 D_4^* + D_3^* D_4^* - K_1 K_1^* \cos^2 \theta - K_2 K_2^* \sin^2 \theta - D_{11} D_{11}^* \sin^2 \theta - D_{33} D_{33}^* \cos^2 \theta - L^2$, $C^* = D_1 D_2 D_3^* + D_1 D_2 D_4^* + D_1 D_3^* D_4^* + D_2 D_3^* D_4^* - (K_2 K_2^* D_1 + D_{11} D_{11}^* D_2 + D_{11} D_{11}^* D_3^* + K_2 K_2^* D_4^*) \sin^2 \theta - (D_{33} D_{33}^* D_1 + K_1 K_1^* D_2 + D_{33} D_{33}^* D_3^* + K_1 K_1^* D_4^*) \cos^2 \theta + L(D_{11}^* D_{33} + D_{11} D_{33}^* + K_1^* K_2 + K_1 K_2^*) \sin \theta \cos \theta - L^2(D_3^* + D_4^*)$, $D^* = D_1 D_2 D_3^* D_4^* + L(K_1^* K_2 D_4^* + K_1 K_2^* D_4^* + D_{11}^* D_{33} D_3^* + D_{11} D_{33}^* D_3^*) \sin \theta \cos \theta - (D_1 D_3^* D_{33} D_{33}^* + K_1 K_1^* D_2 D_4^*) \cos^2 \theta - (D_2 D_3^* D_{11} D_{11}^* + K_2 K_2^* D_1 D_4^*) \sin^2 \theta - (K_1 K_2^* D_{11}^* D_{33} + K_1^* K_2 D_{11} D_{33}^*) \cos^2 \theta \sin^2 \theta + K_1 K_1^* D_{33} D_{33}^* \cos^4 \theta + K_2 K_2^* D_{11} D_{11}^* \sin^4 \theta - L^2 D_3^* D_4^*$, where $D_1 = A_{11} \sin^2 \theta + A_{55} \cos^2 \theta$, $D_2 = A_{33} \cos^2 \theta + A_{66} \sin^2 \theta$, $D_3 = B_{66} \cos^2 \theta + B_{77} \sin^2 \theta$, $D_4 = A_{11}^* \sin^2 \theta + A_{33}^* \cos^2 \theta$, $L = (A_{13} + A_{56}) \sin \theta \cos \theta$, $D_{11}^* = \frac{D_{11}}{j_0}$, $D_{33}^* = \frac{D_{33}}{j_0}$, $D_4^* = \frac{D_4}{j_0} + \frac{\xi}{j_0 k^2}$, $K_1^* = \frac{K_1}{jk^2}$, $K_2^* = \frac{K_2}{jk^2}$, $D_3^* = \frac{\chi}{jk^2} + \frac{D_3}{j}$, $j_0 = \frac{j_0}{\rho}$.

The four roots of bi-quadratic velocity Eq. (15) correspond to the speeds of propagation of coupled longitudinal displacement (CLD) wave, coupled longitudinal microstretch (CLM) wave, coupled transverse displacement (CTD) wave and coupled transverse microrotational (CTM) wave in the medium. The numerical solution of Eq. (15) and reduced velocity equations in absence of transverse anisotropy and microstretch shows that $v_{CLD} > v_{CTD} > v_{CLM} > v_{CTM}$.

Reflection from a stress-free surface

For an incident coupled longitudinal displacement (CLD) wave at stress free surface $z = 0$, there will be four reflected waves as shown in Fig. 1. The mechanical boundary condition at $z = 0$ are vanishing of the normal component of force stress, the tangential component of force stress, the tangential component of couple stress and the microstretch function, i.e.,

$$t_{33} = 0, \quad t_{31} = 0, \quad m_{32} = 0, \quad \pi_3 = 0. \tag{16}$$

where $t_{33} = A_{13} u_{1,1} + A_{33} u_{3,3} + D_{33} \Phi$, $t_{31} = A_{56} u_{3,1} + A_{55} u_{1,3} + K_1 \phi_2$, $m_{32} = B_{66} \phi_{2,3}$, $\pi_3 = h_3 \Phi + A_{31}^* \Phi_{,1} + A_{33}^* \Phi_{,3}$.

The appropriate displacement components u_1, u_3 , microrotation component ϕ_2 and microstress function Φ are taken as

$$u_1 = A_0 \exp \{ik_1 (x \sin \theta_0 + z \cos \theta_0 - v_1 t)\} + \sum_{j=1}^4 A_j \exp \{ik_j (x \sin \theta_j - z \cos \theta_j - v_j t)\}, \tag{17}$$

$$u_3 = p_1 A_0 \exp \{ik_1 (x \sin \theta_0 + z \cos \theta_0 - v_1 t)\} + \sum_{j=1}^4 p_j A_j \exp \{ik_j (x \sin \theta_j - z \cos \theta_j - v_j t)\}, \tag{18}$$

$$\phi_2 = q_1 A_0 \exp \{ik_1 (x \sin \theta_0 + z \cos \theta_0 - v_1 t)\} + \sum_{j=1}^4 q_j A_j \exp \{ik_j (x \sin \theta_j - z \cos \theta_j - v_j t)\}, \tag{19}$$

$$\Phi = r_1 A_0 \exp \{ik_1 (x \sin \theta_0 + z \cos \theta_0 - v_1 t)\} + \sum_{j=1}^4 r_j A_j \exp \{ik_j (x \sin \theta_j - z \cos \theta_j - v_j t)\}. \tag{20}$$

where $v_i (i = 1, 2, \dots, 4)$ are real speeds of CLD, CTD, CLM and CTM waves, respectively and the expressions for p_l, q_l and $r_l (l = 1, 2, \dots, 4)$ are given in Appendix.

These displacement components, microrotation component and microstress function satisfy boundary conditions (16) if following Snell's laws hold

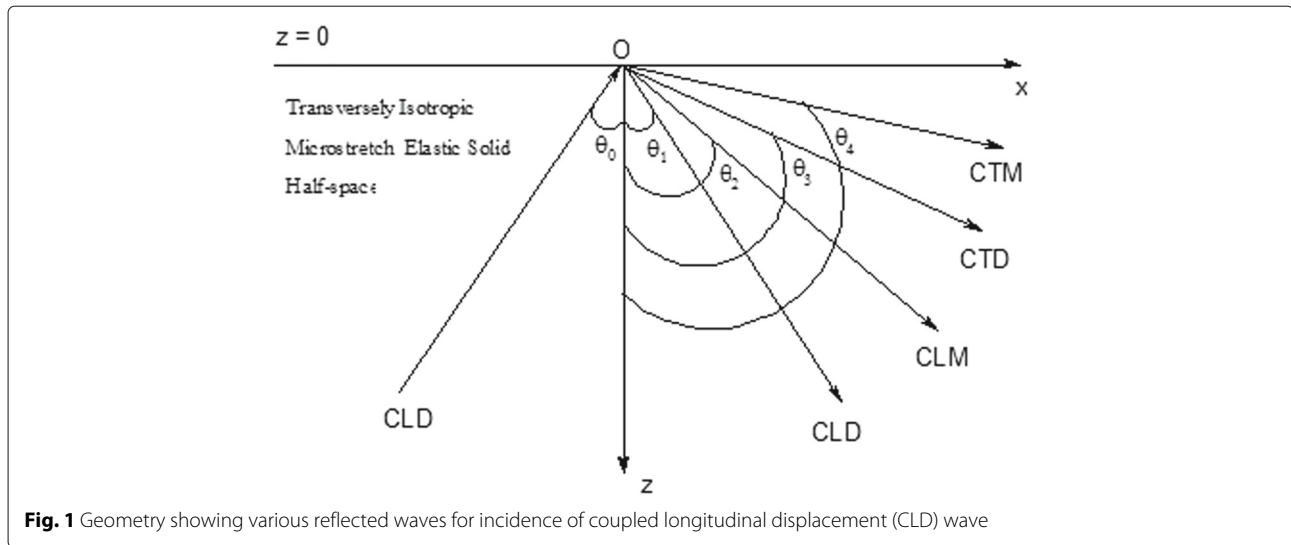
$$k_1 \sin \theta_0 = k_1 \sin \theta_1 = k_2 \sin \theta_2 = k_3 \sin \theta_3 = k_4 \sin \theta_4, \tag{21}$$

$$k_1 v_1 = k_2 v_2 = k_3 v_3 = k_4 v_4 \tag{22}$$

and a non-homogeneous system of four equations in reflection coefficients is obtained as

$$\sum_{j=1}^4 a_{ij} Z_j = b_i, \quad (i = 1, 2, \dots, 4) \tag{23}$$

where $Z_j = \frac{A_j}{A_0}$, ($j = 1, 2, \dots, 4$) are amplitude ratios of reflected CLD, CTD, CTM and CLM waves, respectively,



and

$$a_{1j} = \frac{iA_{13} \sin \theta_0 - ip_j A_{33} \frac{v_1}{v_j} \sqrt{1 - \sin^2 \theta_0 \left(\frac{v_j}{v_1}\right)^2} + D_{33} \frac{r_j}{k_1}}{iA_{13} \sin \theta_0 + ip_1 A_{33} \cos \theta_0 + D_{33} \frac{r_1}{k_1}},$$

$$(j = 1, 2, \dots, 4),$$

$$a_{2j} = \frac{ip_j A_{56} \sin \theta_0 - iA_{55} \frac{v_1}{v_j} \sqrt{1 - \sin^2 \theta_0 \left(\frac{v_j}{v_1}\right)^2} + K_1 \frac{q_j}{k_1}}{ip_1 A_{56} \sin \theta_0 + iA_{55} \cos \theta_0 + K_1 \frac{q_1}{k_1}},$$

$$(j = 1, 2, \dots, 4),$$

$$a_{3j} = \frac{q_j \frac{v_1}{v_j} \sqrt{1 - \sin^2 \theta_0 \left(\frac{v_j}{v_1}\right)^2}}{q_1 \cos \theta_0}, \quad (j = 1, 2, \dots, 4),$$

$$a_{4j} = \frac{ir_j A_{31}^* \sin \theta_0 - ir_j A_{33}^* \frac{v_1}{v_j} \sqrt{1 - \sin^2 \theta_0 \left(\frac{v_j}{v_1}\right)^2} + h_3 \frac{r_j}{k_1}}{ir_1 A_{31}^* \sin \theta_0 + ir_1 A_{33}^* \cos \theta_0 + h_3 \frac{r_1}{k_1}},$$

$$(j = 1, 2, \dots, 4),$$

$$b_1 = -1, \quad b_2 = -1, \quad b_3 = 1, \quad b_4 = -1.$$

The above theoretical analysis reduces for transversely isotropic micropolar elastic case, when $D_{11} = 0$ and $D_{33} = 0$. The above analysis also reduces for transversely isotropic elastic case, when $D_{11} = 0$, $D_{33} = 0$, $K_1 = 0$ and $K_2 = 0$.

Results and discussion

To the best of authors knowledge, the micromechanics based data for transversely isotropic micropolar and microstretch materials is not available in literature. Recent studies on wave propagation in transversely

isotropic micropolar or microstretch media have considered theoretical values of elastic moduli (for example, Gupta and Kumar 2009; Kumar and Gupta (2010a); Kumar and Gupta (2010b); Kumar and Gupta (2012) and Abbas and Kumar 2014). It is reasonable to connect the present theoretical study to polymers, graphite, asphalt, human bones, composite material with reinforced chopped elastic fibres and porous media saturated with gas or inviscid liquid. But so far no experiment with a microstretch interpretation to determine the elastic constants are known on these physical materials. In present study, the relevant values of physical constants (satisfying the inequalities among these constants) of a transversely isotropic composite material modelled as microstretch medium are taken to compute the wave speeds of plane waves and the reflection coefficients of reflected waves.

$$\begin{aligned} A_{11} &= 17.8 \times 10^{11} Nm^{-2}, & A_{33} &= 18.43 \times 10^{11} Nm^{-2}, \\ A_{13} &= 7.59 \times 10^{11} Nm^{-2}, \\ A_{56} &= 1.89 \times 10^{11} Nm^{-2}, & A_{55} &= 4.357 \times 10^{11} Nm^{-2}, \\ A_{66} &= 4.42 \times 10^{11} Nm^{-2}, \\ A_{65} &= 4.32 \times 10^{11} Nm^{-2}, & B_{77} &= 0.278 \times 10^{10} N, \\ B_{66} &= 0.268 \times 10^{10} N, \\ A_{11}^* &= 0.03 \times 10^{11} Nm^{-2}, & A_{33}^* &= 0.04 \times 10^{11} Nm^{-2}, \\ D_{11} &= 0.062 \times 10^{10} N, \\ D_{33} &= 0.063 \times 10^{10} N, & \rho &= 1.74 \times 10^3 Kg m^{-3}, \\ j &= 0.196 m^2. \end{aligned}$$

For these theoretical values of physical constants, the bi-quadratic Eq. (15) is solved numerically for phase speeds of plane waves by using Fortran program of Ferrari's method. For above physical constants, the non-homogeneous system (23) of four equations is also solved numerically to compute the values of amplitude ratios of various reflected waves by using Fortran program of

Gauss elimination method. To check correct implementation of code, the variations of computed phase speeds and amplitude ratios are verified with earlier established results in absence of transverse isotropy and microstretch (Ewing et al. 1957; Achenbach 2003; Singh 2002).

The speeds of plane waves are computed and plotted for range $0^\circ \leq \theta \leq 90^\circ$ of propagation direction in Figs. 2, 3, 4 and 5. The values of speeds shown on y-axis in these figures are without multiplier $\times 10^4$. For transversely isotropic microstretch and transversely isotropic micropolar cases, the variations of speeds of coupled longitudinal displacement (CLD) wave are shown graphically in Fig. 2 by solid and dotted curves, respectively. For transversely isotropic microstretch case (solid curve), the speed of CLD wave varies between $3.055 \times 10^4 \text{ m.s}^{-1}$ and $3.275 \times 10^4 \text{ m.s}^{-1}$. Maximum speed of CLD wave is observed for angle of propagation $\theta = 0^\circ$. The speed of CLD wave decreases to its minimum value $3.055 \times 10^4 \text{ m.s}^{-1}$ at angle of propagation $\theta = 45^\circ$. Thereafter, it increases and attains a value $3.218 \times 10^4 \text{ m.s}^{-1}$ at propagation angle $\theta = 90^\circ$. This change in values of speed of CLD wave with the angle of propagation is due to the presence of transverse isotropy in the medium. This velocity anisotropy of CLD wave is quite significant at angle of propagation $\theta = 45^\circ$. Comparing solid and dotted variations in Fig. 2, it is observed that the values of speed of CLD wave increase at each angle of propagation in presence of microstretch. However, this increase is not equal at each angle of propagation. In absence of transverse isotropy, the speed of CLD wave in both cases becomes equal at each angle of propagation and the increase in speed due to microstretch is also equal at each angle of propagation. This significant difference between microstretch and

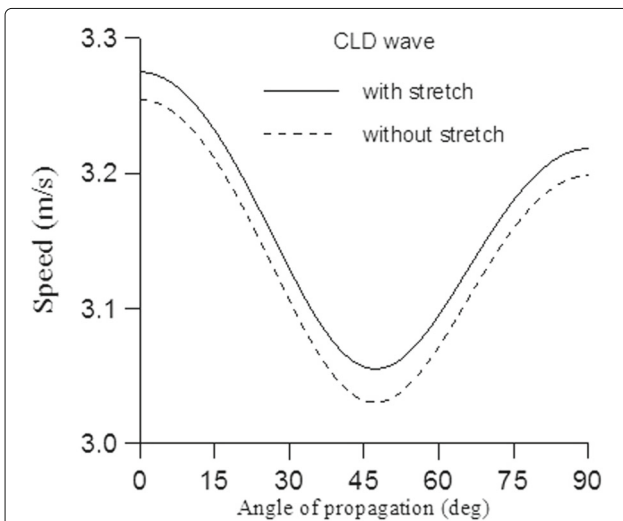


Fig. 2 Variations of the speeds of coupled longitudinal displacement (CLD) wave against the angle of propagation. The values of speed on vertical axis are shown with multiplier $\times 10^4$

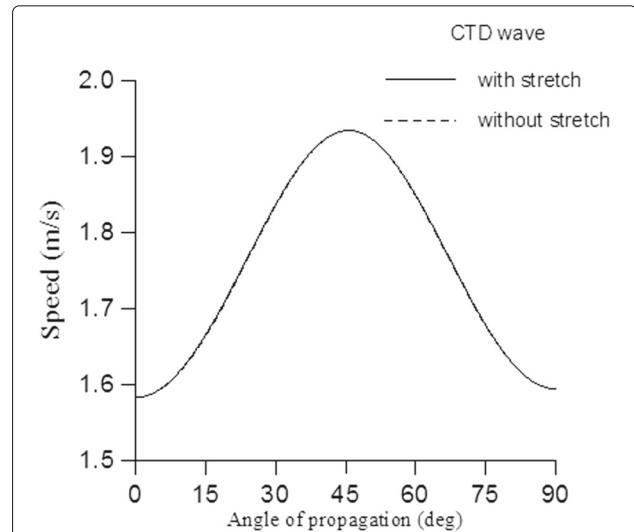


Fig. 3 Variations of the speeds of coupled transverse displacement (CTD) wave against the angle of propagation. The values of speed on vertical axis are shown with multiplier $\times 10^4$

non-microstretch cases is observed due to the strong coupling between longitudinal displacement and longitudinal microstretch fields.

For transversely isotropic microstretch and transversely isotropic micropolar cases, the speeds of coupled transverse displacement (CTD) wave are plotted against the angle of propagation in Fig. 3 by solid and dotted curves, respectively. For transversely isotropic microstretch case, the speed of CTD wave is $1.583 \times 10^4 \text{ m.s}^{-1}$ at propagation angle $\theta = 0^\circ$. It increases to its maximum value

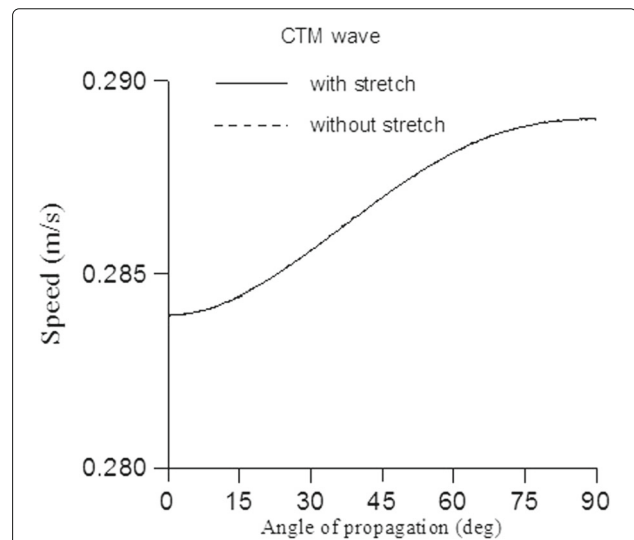
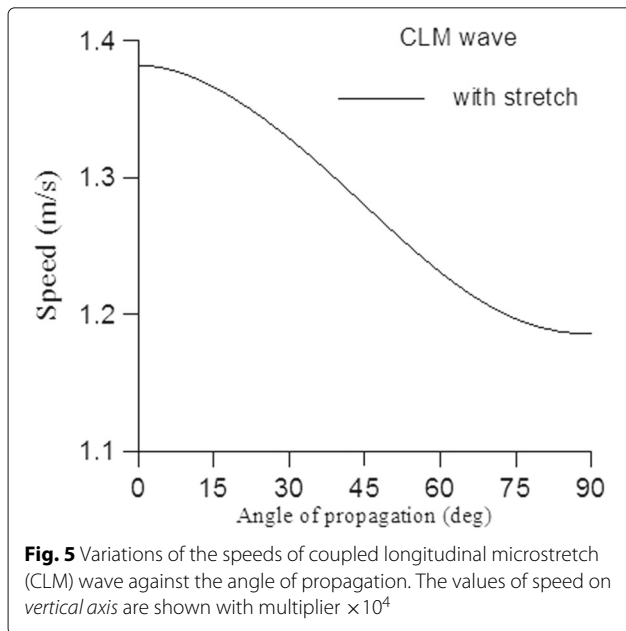


Fig. 4 Variations of the speeds of coupled transverse microrotational (CTM) wave against the angle of propagation. The values of speed on vertical axis are shown with multiplier $\times 10^4$



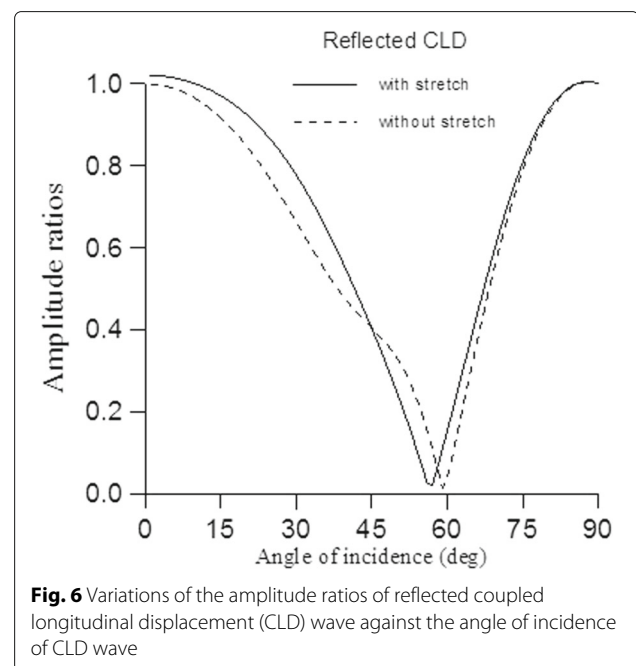
$1.934 \times 10^4 \text{ m.s}^{-1}$ at angle of propagation $\theta = 46^\circ$. Thereafter, it decreases to a value $1.594 \times 10^4 \text{ m.s}^{-1}$ at propagation angle $\theta = 90^\circ$. This significant change in speed of CTD wave in range $0^\circ \leq \theta \leq 90^\circ$ is due to the presence of transverse isotropy in medium. Comparing solid and dotted variations in Fig. 3, it is observed that there is a little effect on the speed of CTD wave due to the presence of microstretch. This small difference in values of speed of CTD wave in two cases is due to weak coupling between transverse displacement and longitudinal microstretch fields. For isotropic cases of microstretch and non-microstretch, the speed of CTD wave is independent of direction of propagation.

Figure 4 shows the variation of speeds of coupled transverse microrotational (CTM) wave against the angle of propagation for microstretch and non-microstretch cases. The speed of CTM wave is $0.284 \times 10^4 \text{ m.s}^{-1}$ at propagation angle $\theta = 0^\circ$. Due to the presence of transverse isotropy in medium, the speed of CTM wave increases with the increase in angle of propagation and attains a maximum value $0.289 \times 10^4 \text{ m.s}^{-1}$ at $\theta = 90^\circ$ to vertical axis. Due to weak coupling between transverse microrotation and longitudinal microstretch, there is no significant difference in values of speeds at each angle of propagation in both cases.

The dependence of speed of coupled longitudinal microstretch (CLM) wave on propagation angle θ is shown graphically in Fig. 5. The speed of CLM wave is $1.382 \times 10^4 \text{ m.s}^{-1}$ at $\theta = 0^\circ$. and it decreases slowly with the increase in angle of propagation and attains to a maximum value $1.186 \times 10^4 \text{ m.s}^{-1}$ at $\theta = 90^\circ$. This change in

speed at each angle of propagation is due to the presence of transverse isotropy in the medium. In transversely isotropic micropolar elastic case, there exists three plane waves, namely, CLD, CTD and CTM waves. In transversely isotropic microstretch elastic medium, CLM is a new wave in addition to CLD, CTD and CTM waves due to coupling between displacement components u_1, u_3 , microrotation component ϕ_2 and microstretch potential Φ .

The amplitude ratios of reflected CLD, CTD, CTM and CLM waves are computed and plotted for range $0^\circ \leq \theta_0 \leq 90^\circ$ of angle of incidence in Figs. 6, 7, 8 and 9. For transversely isotropic microstretch case, the amplitude ratio of reflected CLD wave is obtained as 1.02 at angle of incidence $\theta_0 = 1^\circ$ (near normal incidence). It decreases sharply with the increase in angle of incidence and attains to a minimum value 0.021 at $\theta_0 = 57^\circ$. Thereafter, it increases sharply to value one at $\theta_0 = 90^\circ$ (grazing incidence). This solid variation of amplitude ratio of CLD wave is shown in Fig. 6. The amplitude ratio of reflected CTD wave is obtained as 0.207 at $\theta_0 = 1^\circ$. It decreases sharply to a value 0.0038 at $\theta_0 = 45^\circ$. Thereafter, it increases and attains its maximum value 0.2475 at $\theta_0 = 71^\circ$ and then decreases to zero at $\theta_0 = 90^\circ$ (grazing incidence). This solid variation of CTD wave is shown in Fig. 7. The amplitude ratio of reflected CTM wave is 0.000984 at $\theta_0 = 1^\circ$. It decreases to a value 0.000018 at $\theta_0 = 45^\circ$. Thereafter, it increases and attains a value 0.0007 at $\theta_0 = 65^\circ$ and then decreases to zero at $\theta_0 = 90^\circ$. This solid variation of the amplitude ratios of reflected CTM wave is shown graphically in Fig. 8. The amplitude ratio of reflected CLM wave is 0.3536 at $\theta_0 = 1^\circ$. It



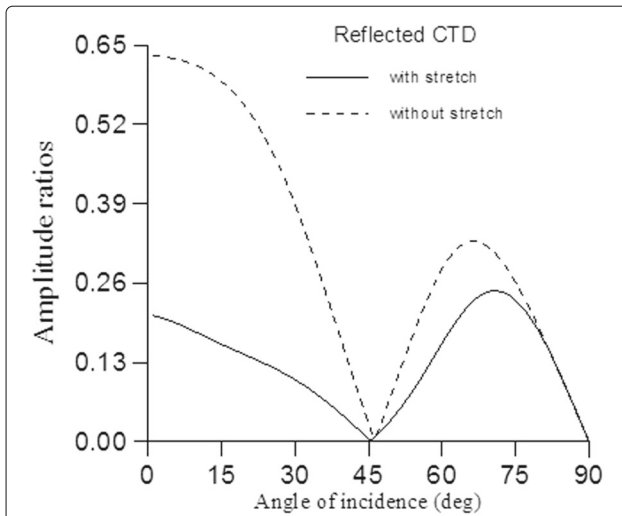


Fig. 7 Variations of the amplitude ratios of reflected coupled transverse displacement (CTD) wave against the angle of incidence of CLD wave

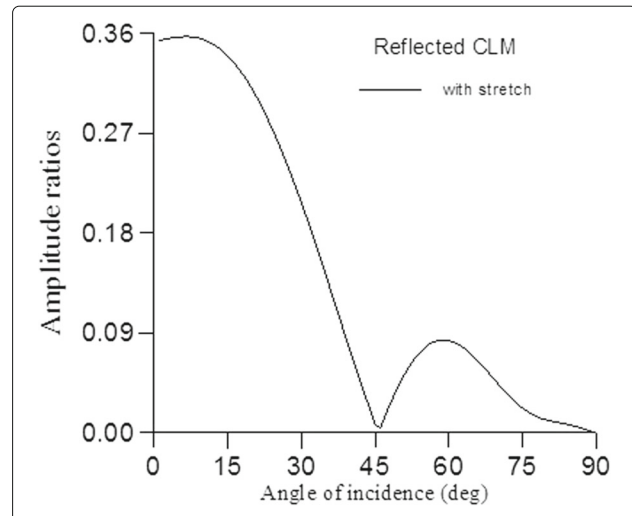


Fig. 9 Variations of the amplitude ratios of reflected coupled longitudinal microstretch (CLM) wave against the angle of incidence of CLD wave

increases slightly to a value 0.3574 at $\theta_0 = 6^\circ$ and then decreases to a value 0.0043 at $\theta_0 = 46^\circ$. Thereafter, it increases and attains a value 0.084 at $\theta_0 = 59^\circ$ and then decreases to zero at grazing incidence $\theta_0 = 90^\circ$. These changes in amplitude ratios of CLD, CTD, CTM and CLM waves are due to the dependence of solutions (amplitude ratios) of homogeneous system (23) on angle of incidence θ_0 and other material parameters. The energy share of reflected CLD, CTD, CTM and CLM waves change at each angle of incidence of incident CLD wave. The dot-

ted variations in Figs. 6 to 9 correspond to transversely isotropic micropolar case. The comparison of solid and dotted curves in these figures show the effect of the presence of microstretch on reflected waves. The extent of this effect depends of coupling between displacement, micro-rotation and microstretch fields. For example, the dotted curve in Fig. 9 is absent as there is no microstretch field in transversely isotropic micropolar elastic case.

Conclusions

From theory and numerical discussion, the following observations are made:

- (1) In x - z plane of a transversely isotropic microstretch elastic medium, four plane waves (CLD, CTD, CLM and CTM waves) propagate with distinct speeds. For a specific material, numerical simulation in presence as well as in absence of microstretch shows that the coupled longitudinal displacement (CLD) wave is fastest wave and the coupled transverse microrotational (CTM) is observed slowest wave. The coupled longitudinal microstretch (CLM) wave is an additional wave due to the presence of microstretch in the medium. For present numerical example, the order in speeds of various plane waves is obtained as ($v_{CLD} > v_{CTD} > v_{CLM} > v_{CTM}$).
- (2) The presence of microstretch in transversely isotropic micropolar elastic solid affects the speeds of plane waves. The coupled transverse displacement (CTD) and coupled transverse microrotational (CTM) waves are least affected due to weak coupling between transverse displacement, transverse microrotation and microstretch fields.

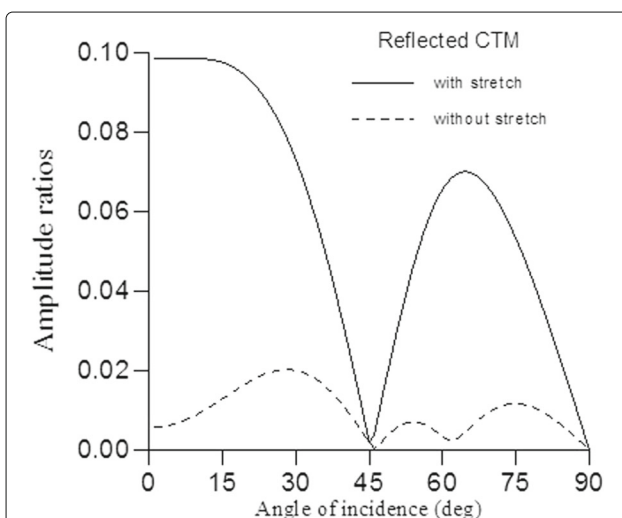


Fig. 8 Variations of the amplitude ratios of reflected coupled transverse microrotational (CTM) wave against the angle of incidence of CLD wave. The solid and dotted variations are plotted after multiplying the original values of amplitude ratios by 100

- (3) Due to the presence of transverse anisotropy in the medium, the speeds of various plane waves depend on angle of propagation direction with vertical axis.
- (4) For incident CLD wave, a non-homogeneous system of four equations in amplitude ratios of various reflected waves is obtained. This system is solved to find amplitude ratios of reflected waves for theoretical values of material parameters.
- (5) The amplitude ratios of various reflected waves depend on angle of incidence of incident CLD wave and material parameters. The energy share of each reflected wave changes at each angle of incidence.
- (6) The presence of microstretch in transversely isotropic micropolar elastic solid affects the amplitude ratios of all reflected waves due to coupling of microstretch fields with displacement and microrotation fields.

The present information though theoretical but may be useful in some possible experiment based problems on wave propagation in a transversely isotropic microstretch elastic medium.

Appendix

The expressions for $p_j, \frac{q_j}{k_j}$ and $\frac{r_j}{k_j}$ ($j = 1, 2, \dots, 4$) are given as

$$p_j = \frac{A_j+B_j}{M_j+N_j}, \frac{q_j}{k_j} = \frac{-i(C_j+D_j)}{M_j+N_j}, \frac{r_j}{k_j} = \frac{-i(E_j+F_j)}{M_j+N_j},$$

where

$$A_j = K_1 K_{1j}^* D_{33} \left[1 - \sin^2 \theta_0 \left(\frac{v_j}{v_1} \right)^2 \right]^{\frac{3}{2}} - K_{1j}^* K_2 D_{11} \sin^2 \theta_0 \left(\frac{v_j}{v_1} \right)^2 \sqrt{1 - \sin^2 \theta_0 \left(\frac{v_j}{v_1} \right)^2},$$

$$B_j = -R_j L_j D_{11} \sin \theta_0 \left(\frac{v_j}{v_1} \right) - P_j R_j D_{33} \sqrt{1 - \sin^2 \theta_0 \left(\frac{v_j}{v_1} \right)^2},$$

$$M_j = -K_2 K_{2j}^* D_{11} \sin^3 \theta_0 \left(\frac{v_j}{v_1} \right)^3 + K_1 K_{2j}^* D_{33} \sin \theta_0 \left(\frac{v_j}{v_1} \right) \left[1 - \sin^2 \theta_0 \left(\frac{v_j}{v_1} \right)^2 \right],$$

$$N_j = R_j Q_j D_{11} \sin \theta_0 \left(\frac{v_j}{v_1} \right) + R_j L_j D_{33} \sqrt{1 - \sin^2 \theta_0 \left(\frac{v_j}{v_1} \right)^2},$$

$$C_j = K_{1j}^* Q_j D_{11} \sin \theta_0 \left(\frac{v_j}{v_1} \right) \sqrt{1 - \sin^2 \theta_0 \left(\frac{v_j}{v_1} \right)^2} + K_{1j}^* L_j D_{33} \left[1 - \sin^2 \theta_0 \left(\frac{v_j}{v_1} \right)^2 \right],$$

$$D_j = K_{2j}^* L_j D_{11} \sin^2 \theta_0 \left(\frac{v_j}{v_1} \right)^2 + K_{2j}^* P_j D_{33} \sin \theta_0 \left(\frac{v_j}{v_1} \right) \sqrt{1 - \sin^2 \theta_0 \left(\frac{v_j}{v_1} \right)^2},$$

$$E_j = K_1 K_{1j}^* Q_j \left[1 - \sin^2 \theta_0 \left(\frac{v_j}{v_1} \right)^2 \right] + K_2 K_{2j}^* P_j \sin^2 \theta_0 \left(\frac{v_j}{v_1} \right)^2,$$

$$F_j = \left(K_1 K_{2j}^* + K_2 K_{1j}^* \right) L_j \sin \theta_0 \left(\frac{v_j}{v_1} \right) \times \sqrt{1 - \sin^2 \theta_0 \left(\frac{v_j}{v_1} \right)^2} + \left(L_j^2 - P_j Q_j \right) R_j,$$

$$P_j = \rho v_j^2 - A_{11} \sin^2 \theta_0 \left(\frac{v_j}{v_1} \right)^2 - A_{55} \left[1 - \sin^2 \theta_0 \left(\frac{v_j}{v_1} \right)^2 \right],$$

$$Q_j = \rho v_j^2 - A_{66} \sin^2 \theta_0 \left(\frac{v_j}{v_1} \right)^2 - A_{33} \left[1 - \sin^2 \theta_0 \left(\frac{v_j}{v_1} \right)^2 \right],$$

$$R_j = \rho v_j^2 - \frac{B_{77}}{j} \sin^2 \theta_0 \left(\frac{v_j}{v_1} \right)^2 - \frac{B_{66}}{j} \left[1 - \sin^2 \theta_0 \left(\frac{v_j}{v_1} \right)^2 \right] - \frac{\chi}{j k_j^2},$$

$$L_j = \left(A_{13} + A_{56} \right) \sin \theta_0 \left(\frac{v_j}{v_1} \right) \sqrt{1 - \sin^2 \theta_0 \left(\frac{v_j}{v_1} \right)^2},$$

$$K_{1j}^* = \frac{K_1}{j k_j^2}, \quad K_{2j}^* = \frac{K_2}{j k_j^2}.$$

Abbreviations

CLD: Coupled Longitudinal Displacement; CLM: Coupled Longitudinal Microstretch; CTD: Coupled Transverse Displacement; CTM: Coupled Transverse Microrotational

Funding

The work is not funded by any agency.

Availability of data and materials

The micromechanics based data for a transversely isotropic microstretch material is not available in literature. The relevant theoretical values of physical constants are used to compute the speeds and reflection coefficients.

Competing interests

The authors declare that they have no competing interests.

Authors' contributions

Both the authors contributed to preparation of the paper. All authors read and approved the final manuscript.

Publisher's Note

Springer Nature remains neutral with regard to jurisdictional claims in published maps and institutional affiliations.

Received: 15 December 2016 Accepted: 14 April 2017

Published online: 26 April 2017

References

Abbas IA, Kumar R (2014) Interaction due to a mechanical source in transversely isotropic micropolar media. *J Vibrot Control* 20:1663–1670

Abubakar I (1962) Free vibrations of a transversely isotropic plate. *Quart J Mech Appl Math* 15:129–136

Achenbach JD (2003) *Wave Propagation in Elastic Solids*, A volume in North-Holland Series in Applied Mathematics and Mechanics. ISBN:978-0-7204-0325-1

Askar A (1972) Molecular crystals and the polar theories of continua. Experimental values of material coefficients for KNO₃. *Int J Eng Sci* 10:293–300

Bazant ZP, Christensen M (1972) Analogy between micropolar continuum and grid frameworks under initial stress. *Int J Solids Struct* 8:327–346

Ciarletta M (1999) On the bending of microstretch plates. *Int J Eng Sci* 37:1309–1318

- Daley PF, Hron F (1977) Reflection and transmission coefficients for transversely isotropic media. *Bull Seismol Soc Am* 67:661–675
- De Bellis ML, Addressi D (2014) A micromechanical approach for the micropolar modeling of heterogeneous periodic media. *Frattura ed Integrità Strutturale* 29:37–48
- Eringen AC (1971) Micropolar elastic solids with stretch. *Ari Kitabevi Matbassi* 24:1–9
- Eringen AC (1990) Theory of thermo-microstretch elastic solid. *Int J Eng Sci* 28:1291–1296
- Eringen AC (1999) *Microcontinuum Field Theories- Volume 1: Foundations and Solids*. Springer-Verlag, New York
- Eringen AC (2001) *Microcontinuum Field Theories - Volume 2: Fluent Media*. Springer-Verlag, New York
- Eringen AC (2004) Electromagnetic theory of microstretch elasticity and bone modelling. *Int J Eng Sci* 42:231–242
- Ewing WM, Jardetzky WS, Press F (1957) *Elastic Waves in Layered Media*. McGraw-Hill Book Company, New York
- Fischer-Hjalmars I (1981) On the validity of the continuum description of molecular crystals. *Int J Eng Sci* 19:1765–1773
- Fischer-Hjalmars I (1982) Micropolar phenomena in ordered structures. In: Brulin O, Hsieh RKT (eds). *Mechanics of Micropolar Media*. World Scientific, Singapore. pp 1–33
- Galich PI, Slesarenko VY, Rudykh S (2016) Shear wave propagation in finitely deformed 3D fiber-reinforced composites. *Int J Solids Struct*. doi:10.1016/j.ijsolstr.2016.12.007
- Galich PI, Fang NX, Boyce MC, Rudykh S (2017) Elastic wave propagation in finitely deformed layered materials. *J Mech Phys Solids* 98:390–410
- Gauthier RD, Jahsmann WE (1975) A quest for micropolar elastic constants. *J Appl Mech* 42:369–374
- Gauthier RD (1982) Experimental investigations of micropolar media. In: Brulin O, Hsieh RKT (eds). *Mechanics of Micropolar Media*. World Scientific, Singapore. pp 395–463
- Gupta RR, Kumar R (2009) Analysis of wave motion in a micropolar transversely isotropic medium. *J Solid Mech* 1:260–270
- Hassonpour S, Heppeler GR (2017) Micropolar elasticity theory: a survey of linear isotropic equations, representative notations, and experimental investigations. *Math Mech Solids* 22:224–242
- Ilesan D, Pompie A (1995) On the equilibrium theory of microstretch elastic solids. *Int J Eng Sci* 33:399–410
- Keck E, Armenkas AE (1971) Wave propagation in transversely isotropic layered cylinders. *ASCE J Eng Mech* 2:541–555
- Kiris A, Inan E (2008) On identification of microstretch elastic moduli of materials by using vibration data of plates. *Int J Eng Sci* 46:585–597
- Kumar R, Singh R, Chadha TK (2003) Plane strain problem in microstretch elastic solid. *Sadhana* 28:975–990
- Kumar R, Ahuja S, Garg SK (2004) Rayleigh waves in isotropic microstretch thermoelastic diffusion solid half space. *Latin Am J Solids Struct* 11:299–319
- Kumar R, Gupta RR (2010a) Reflection of waves in transversely isotropic micropolar thermoelastic half-space. *Canadian Appl Math Quart* 18:393–413
- Kumar R, Gupta RR (2010b) Propagation of waves in transversely isotropic micropolar generalized thermoelastic half-space. *Int Commun Heat Mass Transf* 37:1452–1458
- Kumar R, Gupta RR (2012) Plane waves reflection in micropolar transversely isotropic generalized thermoelastic half-space. *Math Sci* 6:1–7
- Kushwaha MS, Halevi P, Dobrzynski L, Djafari-Rouhani B (1993) Acoustic band structure of periodic elastic composites. *Phys Rev Lett* 71:2022–2025
- Lakes RS (1991) Experimental micro mechanics methods for conventional and negative Poisson's ratio cellular solids as Cosserat continua, adapted from. *J Eng Mater Tech* 113:148–155
- Marin MA (2010) Domain of influence theorem for microstretch elastic materials. *Nonlinear Anal Real World Appl* 11:3446–3452
- Niu B, Yan J (2016) A new micromechanical approach of micropolar continuum modeling for 2-D periodic cellular material. *Acta Mechanica Sinica* 32:456–468
- Nowinski JL (1993) On the surface waves in an elastic micropolar and microstretch medium with nonlocal cohesion. *Acta Mech* 96:97–108
- Othman MIA, Jahangir A (2015) Plane waves on rotating microstretch elastic solid with temperature dependent elastic properties. *Appl Math Informat Sci* 9:2963–2972
- Payton RG (1992) Wave propagation in a restricted transversely isotropic elastic solid whose slowness surface contains conical points. *Quart J Mech Appl Math* 45:183–197
- Pouget J, Askar A, Maugin GA (1986) Lattice models for elastic ferroelectric: microscopic approach. *Phys Rev B* 33:6304–6319
- Rudykh S, Boyce MC (2014) Transforming wave propagation in layered media via instability-induced interfacial wrinkling. *Phys Rev Lett* 112:034301
- Rudykh S, deBotton G (2012) Instabilities of hyperelastic fiber composites: micromechanical versus numerical analyses. *J Elast* 106:123–147
- Rytov SM (1956) Acoustical properties of a thinly laminated medium. *Sov Phys Acoust* 2:68–80
- Sharma JN, Kumar S, Sharma YD (2007) Propagation of Rayleigh surface waves in microstretch thermoelastic continua under inviscid fluid loadings. *J Thermal Stress* 31:18–39
- Sharma JN, Kumar S, Sharma YD (2009) Effect of micropolarity, microstretch and relaxation times on Rayleigh surface waves in thermoelastic solids. *Int J Appl Math Mech* 5:17–38
- Sharma S, Sharma K, Bhargava RR (2014) Plane waves and fundamental solution in an electro-microstretch elastic solids. *Afrika Matematika* 25:483–497
- Singh B (2002) Reflection of plane waves from free surface of a microstretch elastic solid. *J Earth System Sci* 111:29–37
- Singh B, Sindhu R, Singh J (2015) Rayleigh surface waves in a transversely isotropic microstretch elastic solid half space. *J Multidiscipl Eng Sci Tech* 7:1742–1747
- Singh D, Rani N, Tomar SK (2016) Dilatational waves at a microstretch solid/fluid interface. *J Vibr Control*
- Suvalov AL, Poncelet O, Deschamps M, Baron C (2005) Long-wavelength dispersion of acoustic waves in transversely inhomogeneous anisotropic plates. *Wave Motion* 42:367–382
- Yang JFC, Lakes RS (1982) Experimental study of micropolar and couple-stress elasticity in bone in bending. *J Biomech* 15:91–98

Submit your manuscript to a SpringerOpen® journal and benefit from:

- Convenient online submission
- Rigorous peer review
- Immediate publication on acceptance
- Open access: articles freely available online
- High visibility within the field
- Retaining the copyright to your article

Submit your next manuscript at ► springeropen.com